Dynamic analysis of a flexible multibody system

Jang-Soo Chae[1,#], Taw-Won Park[2] and J. Kim[3]

1 Space Development & Research Center, Korea Aerospace Industries, Ltd. Daejeon, South Korea
2 School of Mechanical Engineering & Industrial Engineering, Ajou University, Seoul, South Korea
3 GNC Group Swales Aerospace Inc., 5050 Power Mill Road Beltsville MD, USA
Corresponding Author / E-mail: jschae@koreaaero.com, TEL: +82-42-939-3571, FAX: +82-2-939-3500

KEYWORDS : Component mode synthesis, Normal mode, Constraint mode, Attachment mode, Joint reaction forces

In the dynamic analysis of a mechanism, if one or more of the components are flexible, then the simulation will not be accurate because of the violation of the rigid body assumption. Mode shapes are used to represent the dynamic behavior of an elastic structure. A modal synthesis method which uses a combination of normal modes, constraint modes, and attachment modes, was used to represent effectively the elastic deformation of a flexible multibody.
Since the combination of these modes should be different for each type of connecting part, the modal synthesis method was studied for the various types of interconnecting joints. In addition, the analysis procedure for the flexible body was explained. A satellite system with flexible solar panels was chosen as an example to show the effectiveness of the proposed method.

Manuscript received: Mach 31, 2004 / Accepted: January 7 2005

1. Introduction

Flexible multibody systems such as spacecrafts, robot manipulators, and industrial machinery are composed of both rigid and elastic bodies. Most of the simulation methods for elastic deformation employ the component mode synthesis (CMS) method.

Deformation modes and corresponding modal coordinates are used in the CMS method to capture the elastic effect of the flexible component in the system. Normal modes are used to account for the structure's general behavior while static modes, like constraint modes and attachment modes, are used to capture the local joint induced deformation effectively. The selection of these modes affects the accuracy of the simulation results. However, it is a very difficult problem to decide the number and type of modes that should be used to properly represent a flexible structure.

In this paper, the results of a model with normal modes are used to select the proper number of static modes and their boundary conditions.

The number of proper normal modes is decided using a convergence test which compares the results of a small and large number of normal modes. A step by step procedure for the flexible body analysis is explained with an example problem of a satellite system.

2. Modal Synthesis Method and flexible Body Analysis

2.1 Types of modes

A typical flexible component is shown in Fig. 1. The global position of a point **p** can be represented as

$$\mathbf{r}^p = \mathbf{r} + \mathbf{A}(\mathbf{S}_0'^p + \mathbf{u}) \tag{1}$$

where **r** is the global position vector of the body reference center, **A** is the transformation matrix from the body reference frame to the global inertial frame, $\mathbf{S}_0'^p$ is the initial position vector of the point **P** from the body reference center, and **u** is the displacement vector due to deformation. The displacement vector **u** can be approximated by a linear combination of deformation modes like equation (2).

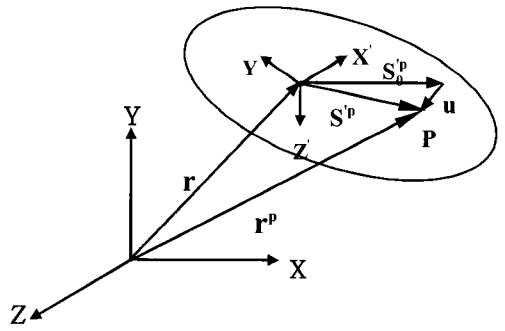

Fig.1 Global displacement of a point p in an elastic component

$$\mathbf{u} = \sum_{i=1}^{M} \phi_i \eta_i \tag{2}$$

where ϕ_i is a modal vector and η_i is the corresponding modal coordinate. The individual M mode should be linearly independent to each other. An elastic component can be described by the second

order matrix differential equation of the form

$$\mathbf{M}_{nn}\ddot{\mathbf{x}}_n + \mathbf{K}_{nn}\mathbf{x}_n = \mathbf{f}_n \quad (3)$$

where $\mathbf{x}_n$ denotes n×1 displacement vector, $\mathbf{f}_n$ denotes n×1 force vector, and $\mathbf{M}_{nn}$ and $\mathbf{K}_{nn}$ represent n×n mass and stiffness matrices respectively. By using Eqn.(3), normal modes can be obtained by solving an eigenvalue problem of the form

$$(\mathbf{K}_{nn} - \omega^2 \mathbf{M}_{nn})\phi_n = 0 \quad (4)$$

Normal modes are used to account for the general elastic deformation of the flexible structures. If a large force is imposed at a nodal coordinate, then the static mode is more effective. Attachment modes and constraint modes are two types of static modes. The constraint mode is obtained by imposing a unit displacement on one of the nodal coordinates, and the attachment mode is obtained by imposing a unit force on one of the nodal coordinates.

Those two types of modes generate similar results. All used normal modes and static modes must be normalized to have the same magnitude and to reduce the numerical, error and orthogonalized to be independent each other.

Differential algebraic equations(DAE) of motion for considering flexible effect are described in Appendix 1.

2.2 Boundary conditions and mode selection

To obtain deformation modes of the elastic component, boundary conditions have to be applied. Usually, nodal coordinates of interconnected joints are selected as boundary conditions. A few of the lowest frequency for normal vibration modes have been used in previous literatures. Some literatures suggest that the number of normal modes can be selected up to the mode whose frequency is twice the interested frequency. In this study, a convergence test is applied to decide proper set of normal modes. To select the proper set of static modes, analysis results have to be examined. Since most mechanical systems are over constrained resulting in redundancy, if only rigid bodies are used, the reaction forces of all joints cannot be obtained. So the result of a model with normal modes is used. With this information, the static mode set can be decided.

2.3 Analysis procedure

First, a rigid body model has to be prepared. Since most flexible components are over constrained, rigid body analysis cannot provide all the information about the reaction forces of each interconnected joint. Therefore, normal modes are used for the elastic component. At this stage, all interconnected joints are used as fixed boundary conditions. The results of flexible body analysis highly depend on the accuracy of the used modes, so the used normal modes have to be verified carefully. Analysis of the results will provide reaction force information for all the interconnected joints. Constraints with small reaction forces do not have to be considered as the static mode set. On the other hand, constraints with large reaction forces are used as static modes. Finally, normal modes and static modes are combined to calculate the elastic deformation of the elastic component.

3. Numerical Simulation and Test

Fig. 3 shows a satellite system with 6 solar panels. Initially, panels are stowed to the main body. During the deployment process, when the panel reaches at a designed angle, the panel is locked. At this moment, a large impact force is applied to the body. This may cause structural damage and affect the control of the satellite. So a reliable dynamic model of the deployment system is required.

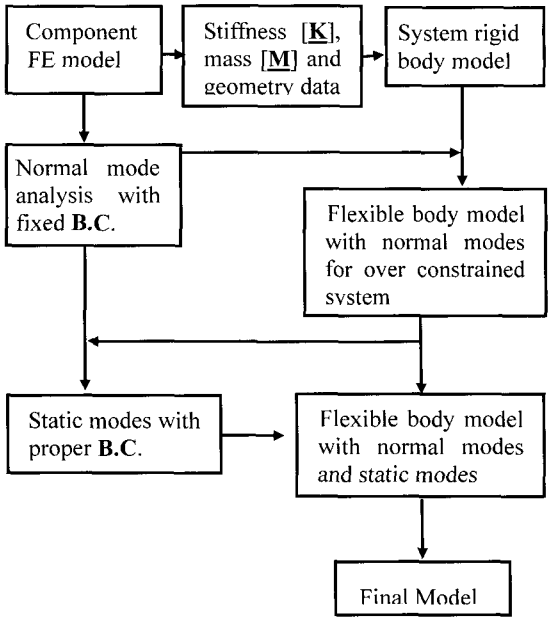

Fig. 2 Flow diagram of flexible multibody analysis

Solar panels are relatively flexible, and rotational motion is generated with many strain energy hinges which have nonlinear characteristics. To model strain energy hinges, revolute joints with rotational springs can be used. But the model will become an over constrained system if only rigid bodies are used.

Dynamic simulation model is shown in Fig. A1 and A2 of Appendix 2.

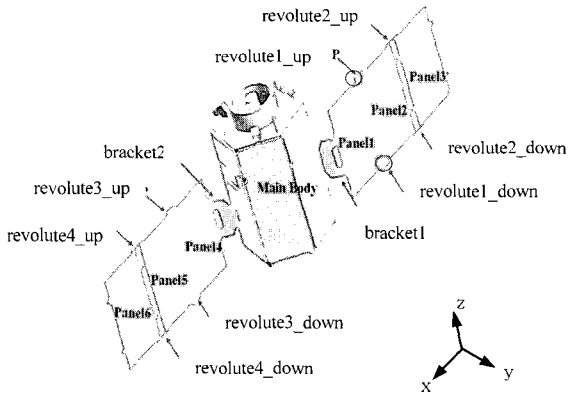

Fig. 3 A satellite system for multibody dynamics

Thus, the analysis results of a model with only rigid bodies cannot supply the joint reaction forces of all the hinges due to redundancy in the model. In addition, elastic energy of the panel may be significant in the calculation of reaction forces on the joints. So the panels were modeled as flexible bodies. The method explained in the previous section was applied to the system. The moments of inertia of the satellite(Ixx, Iyy, Izz) were 3,490, 3,637 and 1,679 $lb_f \cdot in^2$ and those of solar panel were 7.45, 9.58 and 2.14 $lb_f \cdot in^2$

3.1 Selection of Modes

The main body and two yokes, which connect the main body and two adjacent panels were modeled as rigid bodies, and four solar panels were modeled as flexible bodies. All four panels had the same geometry and had several layers of composite materials. The property is shown in Table A1 of Appendix 2.

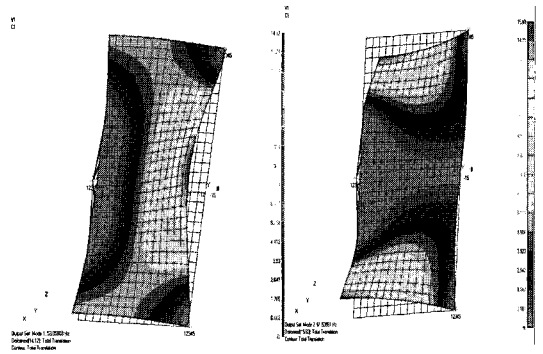

Fig. 4 Panel mode shape 53.0Hz(1st), 61.5Hz(2nd)

The thin shell linear quadrilateral elements and composite materials were used for the finite element model of the solar panel. NASTRAN 70.5 was used for the finite element analysis of the solar panel(Fig. 4, Appendix 2) and DMAP was used to calculate static modes, and DADS was used for dynamic analysis of the satellite. All kinematic constraints were used as boundary conditions for the normal mode analysis.

Thirty normal modes were used for each panel. Fig. 5 shows reaction forces on the R1 revolute joint. The result shows that the x and y direction forces are significant and other direction forces are negligible. Thus x, y coordinates of the node where the R1 joint was connected were chosen to calculate static modes. The R2 joint also showed similar results. So panel 2 had four static modes. Table 1 shows boundary conditions and forcing conditions of static modes decided for panel 2.

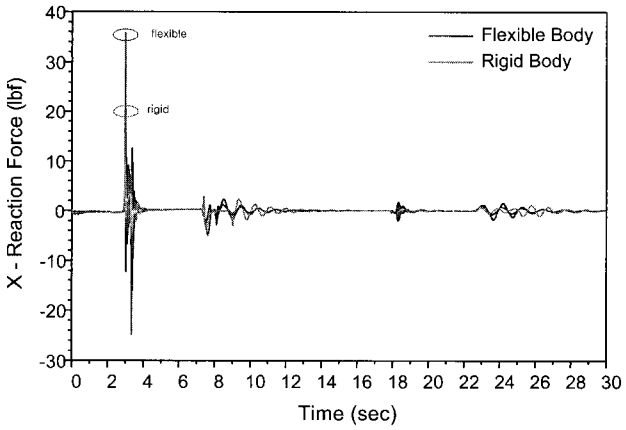

Fig. 5 Response of reaction force(X) on R3 joint

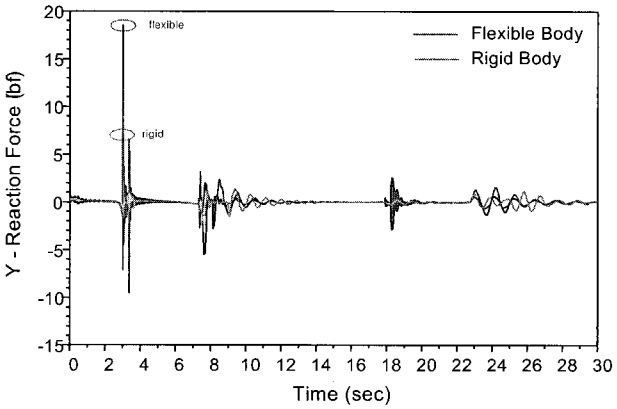

Fig. 6 Response of reaction force(Y) on R3 joint

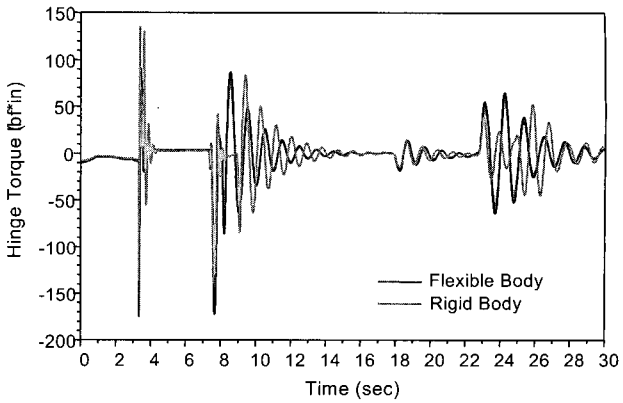

Fig. 7 Response of reaction torque on R3 joint

Table 1 Loads and boundary conditions for static modes on panel 2

case	Joint	X	Y	Z	RX	RY	RZ
1	revolute 3	1	0	0	0	0	free
	revolute 4	0	0	0	0	0	free
2	revolute 3	0	1	0	0	0	free
	revolute 4	0	0	0	0	0	free
3	revolute 3	0	0	0	0	0	free
	revolute 4	1	0	0	0	0	free
4	revolute 3	0	0	0	0	0	free
	revolute 4	0	1	0	0	0	free

Even though thirty normal modes were obtained from the normal mode analysis, if the simulation result s not improved with more normal modes then a smaller number of normal modes can be used. Fig. 6 shows the analysis results with 5 and 10 normal modes.

The result with two normal modes is very close to the result with 10 normal modes. But simulation time is increased if more modes were used in the model. Thus, two normal modes and four static modes were chosen to represent elastic deformation of the panel 2. Proper mode set was decided for the other panels using the same procedure.

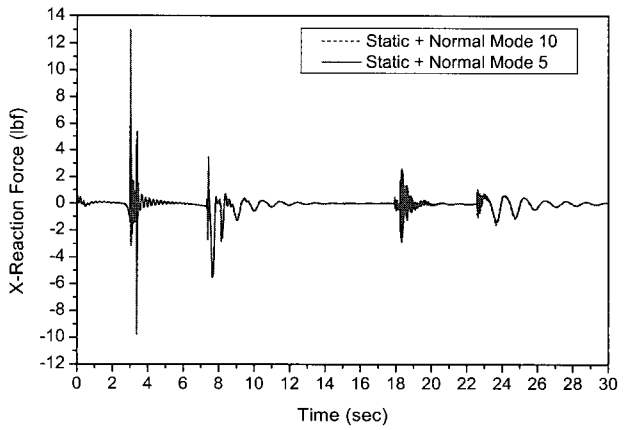

Fig. 8 X-directional reaction force on R1 joint

3.2 Analysis Results

The X-directional force on the R1 revolute joint is shown in Fig. 9. There is difference between rigid and flexible body dynamics of joint reaction force about revolute joint connecting fixture to yoke panel in Fig.3.

All revolute joint were replaced by cylindrical joints to consider motion due to the cable tension and gravity.

As shown in Fig. 9, flexible model has larger reaction force than rigid model. It is very important to design hinge property.

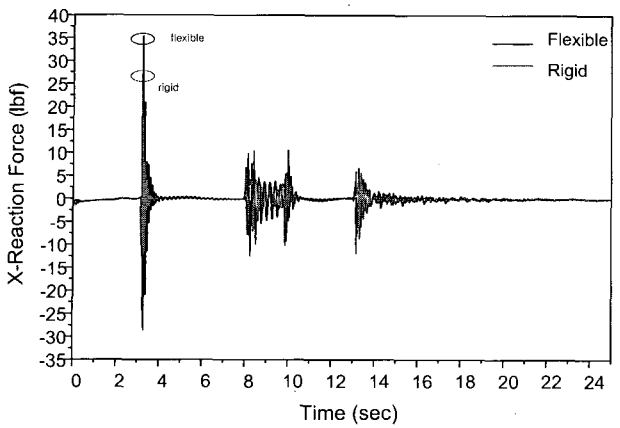

Fig. 9 X - directional reaction force on R1 joint

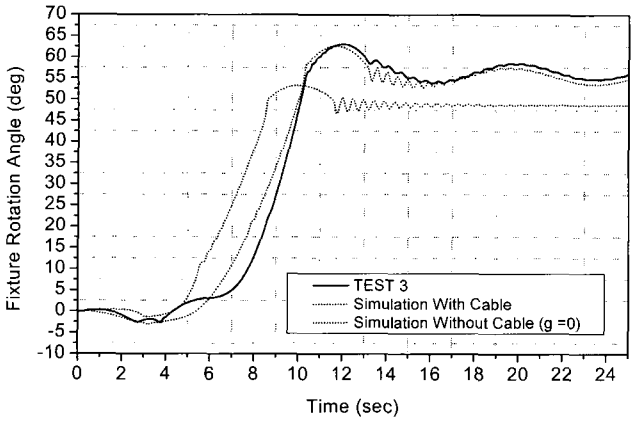

Fig. 10 Yaw angle of the satellite main body

Fig. 10 compares the yaw angle of the main body with cable and not. It is found that deployment motion is considerably different from that with gravity-free state. It shows that the flexible model is required to design an accurate control system rather than rigid model.

3.3 Test Results

It is necessary to check the performance of deployment test on the ground without vertical acceleration, i.e., gravity-free state (zero g). Fig. 11 shows the deployment test equipment with counter weight and cable considering gravity-free state on the ground. This test equipment was set to verify the reliability of dynamic analysis. Solar panel was hanging from the ceiling by wire cable. We pick up the response of hinge rotation using the accelerator on root. However, the effect of gravity is not fully compensated to this test device during the deployment test.

As shown in Fig. 10, the results of test and simulation are different due to the cable for considering. It comes from the nonlinear features such as balance of test equipment, damping, cable length and its tension, friction and contact with test fixture. Tension effect of the cable was considered in dynamic analysis model sufficiently, but the effect of friction was not included in this model.

Fig. 12 shows the response of rotation hub angle via time with respect to the cable length of 12 and 18 meters. It shows the different motion with respect to the cable length. The longer cable makes the slower response. It is found that the different motion is that with gravity-free state

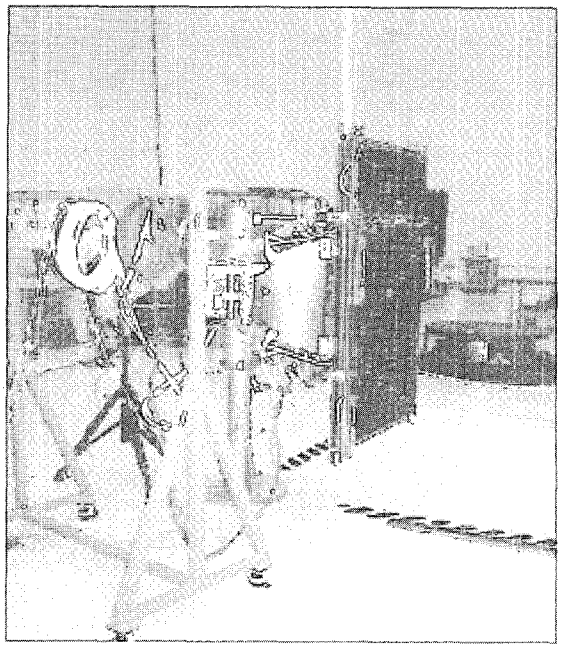

Fig. 11 Test equipment of solar array panel deployment with hinge mechanism

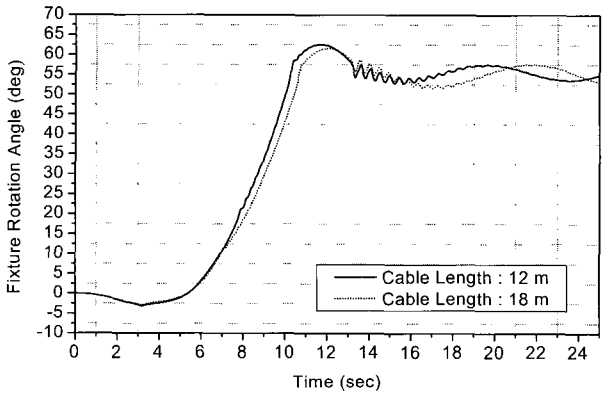

Fig. 12 Main body rotation angle with respect to cable length

4. Conclusions

In this study, an analysis of the system with elastic components was presented. In particular, the method to select the proper set of deformation modes and boundary condition for solving the redundant problem was shown.

The reliability of the flexible body model was very important in the design of strain energy hinges and control systems of the space structure. Thus, a satellite system was modeled as the multibody system with flexible bodies using the proposed method. This method can be applied to any mechanical system where flexibility for the component is important.

REFERENCES

1. Spanos, J.T. and Tsuha, W.S., "Selection of Component Modes for Flexible Multibody Simulation," Journal of Guidance 14:2, pp. 278-286, 1991.

2. Parviz, E. Nikravesh, "Computer-Aided Analysis of Mechanical Systems," Prentice-hall, Inc., 1988.

3. Craig, R.R.Jr., "Structural Dynamics," Wiley, 1981.

4. Shin, S.S., Yoo, W.S. and Tang, J., "Effect of Mode Selection, Scaling, and Orthogonalization on the Dynamic Analysis of Flexible Multibody Systems," Mechanics of Structures and Machines, 21:4, pp. 507-527, 1993.

5. Kim, S.S. and Haug E.J., "Selection of Deformation Modes for Flexible Multibody Dynamics," Mechanics of Structures and Machines, 18:4, pp. 565-586, 1990.

6. Michae,l R. and Mark, M., "MSC/NASTRAN Quick Reference Guide Version 68," The MacNeal-Schwendler Corporation, 1994.

7. DADS 9.5 Reference Manual, LMS, 1990.

Appendix 1: Dynamic Equations

The kinematics and driving constraints of the multibody dynamic system can be written in the form

$$\Phi(q,t)=0 \tag{A1}$$

Where, $q=[q_1^T,q_1^T,\cdots,q_{nb}^T]^T$

Φ : Constraint equation

Then, the variation δq of the system generalized coordinates must satisfy Eqn. (A2).

$$\Phi_q \delta q=0 \tag{A2}$$

The variation equations of the motion of the multibody system can be obtained by summing all bodies and constraints in the system and writing the result in the compact form of Equ. (A3).

$$\delta q^T\{M^*\ddot{q}-Q^*\}=0 \tag{A3}$$

Where

$$\delta q=[\delta q_1^T,\delta q_2^T,\cdots,\delta q_{nb}^T]^T \tag{A4}$$

Augmented state variable vector

$$\ddot{q}=[\ddot{q}_1^T,\ddot{q}_1^T,\cdots,\ddot{q}_{nb}^T]^T \tag{A5}$$

Acceleration vector

$$M^*=diag[M_1,M_2,\cdots,M_{nb}]^T \tag{A6}$$

Augmented mass matrix

$$Q^*=diag[Q_1,Q_2,\cdots,Q_{nb}]^T \tag{A7}$$

Augmented generalized force vector

Eqn. (A3) holds for all δq that satisfy Eqn. (A2) by Farkas lemma, there exist a Lagrange Multiplier Vector λ such that

$$\delta q^T\{M^*\ddot{q}+\Phi_q^T\lambda-Q^*\}=0 \tag{A8}$$

for arbitrary δq, yielding the equation of motion

$$M^*\ddot{q}+\Phi_q^T\lambda-Q^*=0 \tag{A9}$$

The constraint acceleration equation is obtained by taking two derivatives of Eqn. (A1)

$$\Phi_q\ddot{q}=-(\Phi_q\dot{q})_q\dot{q}-2\Phi_{qt}q-\Phi_{tt}\equiv\gamma \tag{A10}$$

Eqn. (A9) and (A10) can be written in matrix form as

$$\begin{bmatrix} M^* & \Phi_q^T \\ \Phi_q & 0 \end{bmatrix}\begin{bmatrix}\ddot{q}\\ \lambda\end{bmatrix}=\begin{bmatrix}Q^*\\ \gamma\end{bmatrix} \tag{A11}$$

Appendix 2: Analysis Model

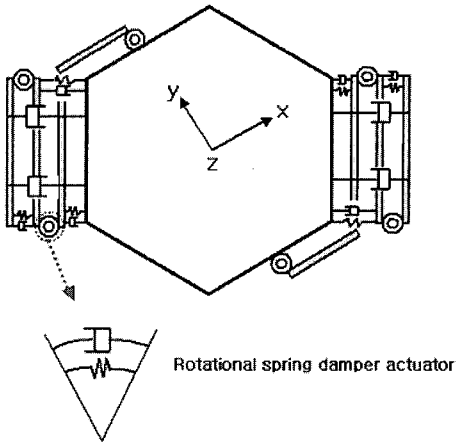

Fig. A1 Satellite dynamic analysis model with spring, damper and actuator (RSDA) type for solar panel

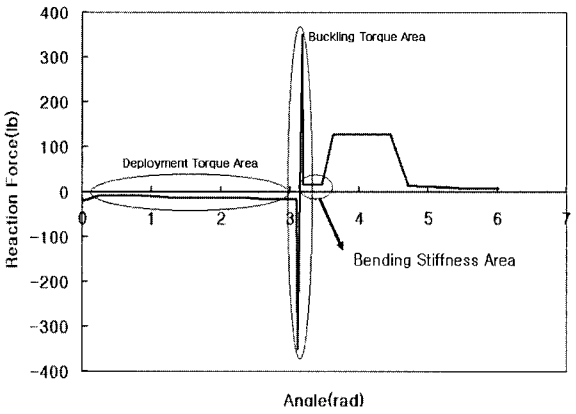

Fig. A2 Deployment toque in the strain energy hinge

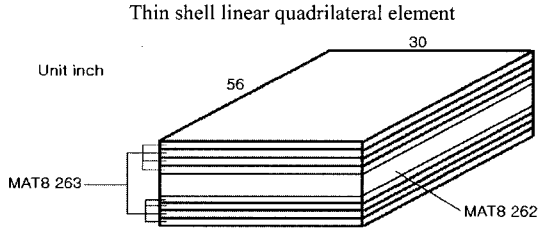

Fig. A3 Shell element type for solar panel

Table A1 Mechanical property for shell element

Mass property	Value	Unit
Density	0.00179	lb/in^3
Poisson ratio, ν_{xy}	0.489	
Mudulus, E_{xx}	4.3366e+4	lb/in^2
Mudulus, E_{yy}	1.6418e+4	lb/in^2
Shear modulus, G_{xy}	2.2248e+4	lb/in^2
Shear modulus, G_{yz}	4.2e+4	lb/in^2
Shear modulus, G_{xz}	2.2e+4	lb/in^2
Thickness(skin)	0.0039	in
Thickness(core)	0.59	in